International Journal of Concrete Structures and Materials
Volume 10, Number 3 Supplement, pp.S43–S52, September 2016
DOI 10.1007/s40069-016-0152-9
ISSN 1976-0485 / eISSN 2234-1315

Evaluation of Bond Properties of Reinforced Concrete with Corroded Reinforcement by Uniaxial Tension Testing

Hyung-Rae Kim[1)], Won-Chang Choi[2)], Sang-Chun Yoon[2),*], and Takafumi Noguchi[3)]

(Received March 22, 2016, Accepted May 20, 2016, Published online June 14, 2016)

Abstract: The degradation of the load-bearing capacity of reinforced concrete beams due to corrosion has a profoundly negative impact on the structural safety and integrity of a structure. The literature is limited with regard to models of bond characteristics that relate to the reinforcement corrosion percentage. In this study, uniaxial tensile tests were conducted on specimens with irregular corrosion of their reinforced concrete. The development of cracks in the corroded area was found to be dependent on the level of corrosion, and transverse cracks developed due to tensile loading. Based on this crack development, the average stress versus deformation in the rebar and concrete could be determined experimentally and numerically. The results, determined via finite element analysis, were calibrated using the experimental results. In addition, bond elements for reinforced concrete with corrosion are proposed in this paper along with a relationship between the shear stiffness and corrosion level of rebar.

Keywords: bond element, corrosion, corrosion weight loss, finite element analysis, shear stiffness.

1. Introduction

In order to determine the load-bearing capacity of a reinforced concrete member, the bond behavior between the concrete and rebar plays an important role in terms of design (Almusallam et al. 1996; Yoon et al. 2000). Various modeling techniques related to bond characteristics are available in the literature (Azad et al. 2010; Dekoster et al. 2003; Stewart 2004). It is well known that corrosion evidently reduces the bond strength between rebar and concrete (Al-Hammoud et al. 2010; Auyeung et al. 2000; Yang et al. 2015). However, the degradation of the bond stress that is due to corrosion has been studied with less attention, and thus, the literature is insufficient to provide clear understanding of the bond characteristics in reinforced concrete members with respect to the distributed area of corrosion in the member and the level of corrosion in the rebar.

Coronelli and Gambarova (2004) employed a bond deterioration index of concrete beam with corrosive conditions in numerical analysis based on non-linear finite element analysis, and the results indicate that bond deterioration significantly influences to determining the residual ductility of a structure. Azad et al. (2007, 2010) used a correction factor to calculate the residual flexural strength of concrete beams with corroded rebar. The earlier research Azad et al. (2007) was found that the theoretical predictions were consistently lower than the actual flexural strength of the beams. To improve the accuracy, the research has been conducted with consideration of the size-effect of rebar diameters Azad et al. (2010).

In a recent study, Imam et al. (2015) used artificial neural networks (ANN) methods to handle the non-linearity in corrosion, coupled with its capability to adaptively learn from hidden patterns in experimental data. But the limited experimental results from Azad et al. (2010) were used for the ANN analysis.

Yang et al. (2015) investigated the effects of corrosion of reinforcing steel on the load-bearing capacity of reinforced concrete beams subjected to the repeated loading. A total of fifteen test specimens were fabricated and evaluated with respect to the deflection, stiffness, bearing capacity and failure shape. The research results confirm the profoundly negative impacts for deflection, flexural rigidity and failure type as the corrosion level increase.

This study pertains to expand the research scopes including the effects of tension stiffening, crack spacing and crack width, bond stress characteristics, and slip. The test variables are four phases of corrosion locations and three types of corrosion levels for each corrosion phase. The related studies were reported by the author Kim et al. (2008). The results from finite element analysis were calibrated with the experimental results. Bond elements conventionally are placed at the interface between the concrete elements and rebar elements in finite element analysis. Bond elements of

[1)]R&D division, Hyundai Engineering & Construction, Yongin-si, Korea.
[2)]Department of Architectural Engineering, Gachon University, Seongnam-si, Korea.
*Corresponding Author; E-mail: scyoon@gachon.ac.kr
[3)]Graduate School of Engineering, The University of Tokyo, Tokyo, Japan.

reinforced concrete with corrosion are proposed based on experimental and numerical analyses.

2. Experimental Program

2.1 Specimen Preparation

The direct tension test was adopted in this study for the experimental program. The direct tensile test can accurately model stress distribution and is relatively simple to set up. However, it is difficult to observe crack spacing and crack widths accurately and also difficult to interpret the data to determine the direct stress. Table 1 presents the test parameters used in this study with the variables for the corroded areas and the level of corrosion. These parameters are considered to be the determinants for the effects on the bond strength between the concrete and corroded reinforcement with respect to the level and area of the corrosion.

Four corrosion areas were used in this study: (1) the overall length of 70 cm ('A', corrosion of entire area, or 'all'), (2) half of the length ('H', corrosion of half the area), (3) 20 cm in the middle of the specimen ('C', corrosion in the center of the specimen), and (4) 20 cm on the side of the specimen ('S', corrosion on the side of the specimen). The results were compared with a control specimen that had no corrosion. Also, three corrosion levels (3, 5, and 10 %) were considered in this study. Those corrosion levels were determined with average corrosion weight loss percentage.

Table 2 presents the mix design and material properties for the concrete mixture used in this study. The reinforcement used in this study was SD 295 A with a diameter of 13 mm (D13). The material properties of this reinforcement are presented in Table 3. Also, each specimen had a square cross-section of 10 mm and was 800 mm in length. A single rebar 1000 mm in length was placed in the middle of the concrete specimen (see Fig. 1).

Table 1 Experiment parameters.

Test parameters	Types
Corrosion area	Corrosion of entire area (A) Corrosion of a half the area (H) Corrosion in the center of specimen (C) Corrosion on the side of the specimen (S)
Corrosion level (average corrosion weight loss)	3, 5, and 10 %

2.2 Test Procedure

Figure 2 shows a schematic drawing of the test set-up used in this study. A pool containing sodium chloride (NaCl) solution was fabricated on the top surface of the concrete and a copper plate was inserted into the pool. A 1 mA/cm^2 electric current was applied to the surface between the rebar and the copper plate. The location of the pool was adjusted based on the effective area of the concrete surface.

The distribution of deformation of corroded rebar cannot be measured directly, so the displacement could be measured at both ends of the concrete specimen and the deformation also must be measured locally. To determine the crack development in the concrete, Pi gauges were installed on the concrete surface. Aluminum channels were fixed to both ends of the concrete specimen and displacement gauges were embedded inside acrylic pipes to measure the overall displacement (see Fig. 3). More detailed information associated with the procedures can be found in elsewhere (Kim 2008).

3. Results and Discussion

3.1 Reinforcement Corrosion and Crack Development

Figure 4 shows the relationship between maximum corrosion weight loss percentages and average corrosion weight loss percentages. Maximum corrosion weight loss percentage was measured every 2.5 cm in highly corroded area and average corrosion weight loss percentage was measured for entire length. The slope of regression line for all specimens is 2.14. The slope of regression line for the entire corrosion series ("A" specimens) is 1.87. These ratio values were decreased with an increase of the length of the corroded area.

Figures 5, 6, and 7 show the corrosion weight loss percentages with respect to the corrosion areas throughout the 'A' and 'H' specimens, respectively, including the crack development of the concrete in terms of the corrosion percentage. The cracks that occurred due to the stress transfer from the rebar to the concrete also are presented in Figs. 5 and 6.

Corrosion cracks in the parallel direction of rebar did not occur when the corrosion weight loss percentage was less than 2.04 %. In addition, corrosion cracks occurred mostly at the surface of the concrete that was in contact with the copper plate or at the side face of the concrete on the specimen.

Table 2 Concrete mix design and material properties.

W/C (%)	S/a (%)	Unit weight (kg/m^3)				AE	f_c' (MPa)	E_c (GPa)
		Water	Cement	Fine aggregate	Coarse aggregate			
55	46.0	170	309	837	1005	Cement ×0.4 %	34.5	27.2

Table 3 Material properties of reinforcement.

Type of reinforcement	F_y, (MPa)	F_u (MPa)	E_s, (GPa)	Elongation (%)
D13 (ϕ 13 mm, 126 mm^2)	461.02	444	196	21.3

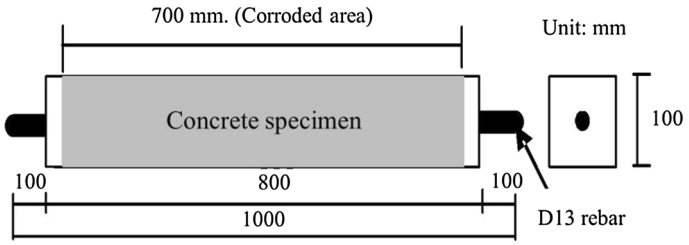

Fig. 1 Test specimen.

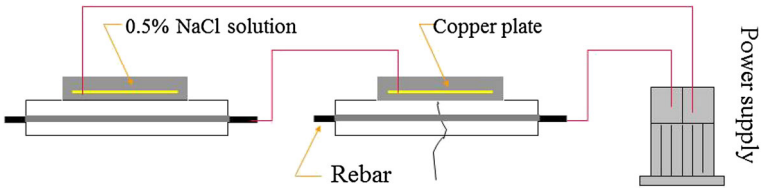

Fig. 2 Electric corrosion method.

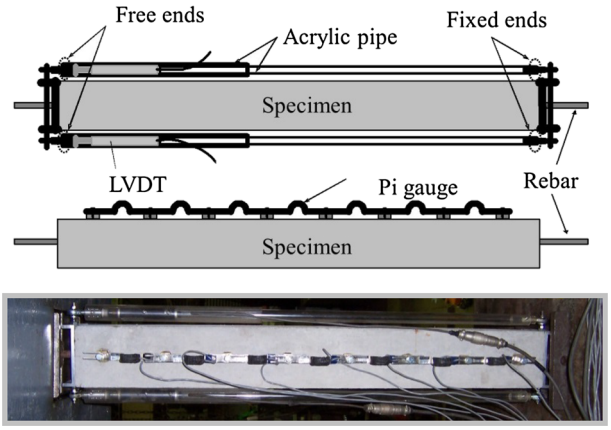

Fig. 3 Gauge installation and test set-up.

For the 'A' corrosion case, longitudinal cracks developed throughout the entire length of the specimen. Transverse cracks were often occurred with an increase in the corrosion weight loss percentage.

For the 'H' local corrosion case, the corrosion crack width was smaller than for the 'A' corrosion case at the same amount of corrosion weight loss percentage.

In the case of 'C' corrosion and 'S' local corrosion, there are more longitudinal corrosion cracks than transverse corrosion cracks. This outcome may be the result of the longitudinal expansion of the local area with a high intensity of corrosion; those areas are very limited and have a shallow concrete cover.

Figure 8 shows the average corrosion weight loss percentages versus maximum corrosion cracks. The corrosion

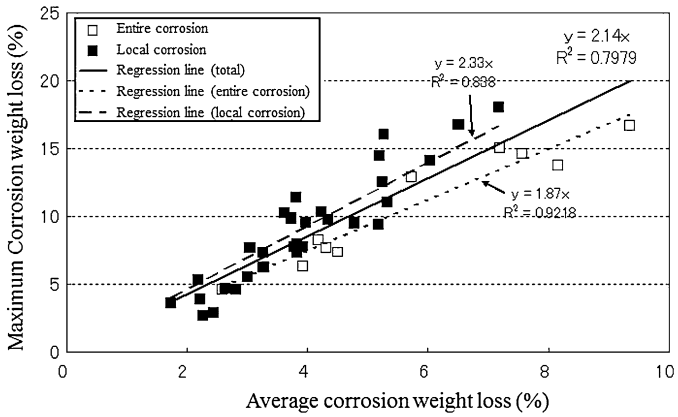

Fig. 4 Maximum corrosion weight loss percentages versus average corrosion weight loss percentages.

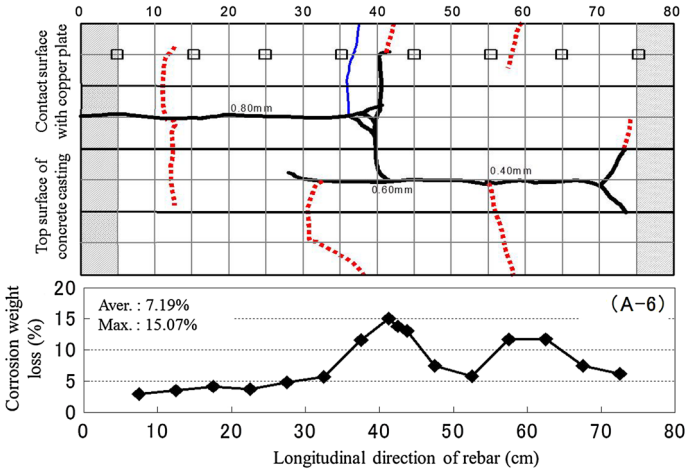

Fig. 5 Distribution of corrosion and cracks for the 'A' specimen with all corrosion.

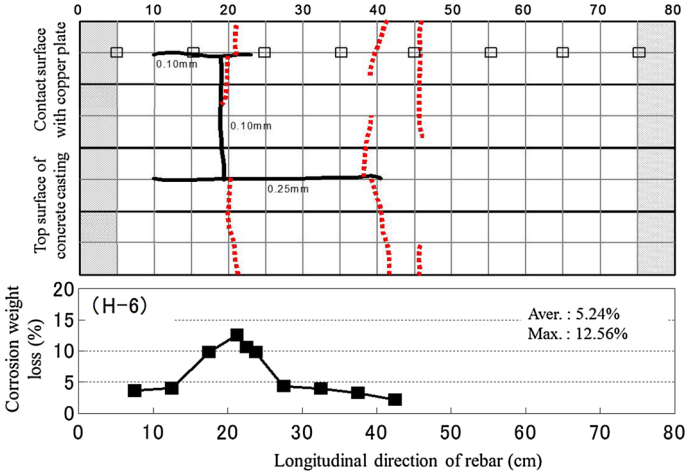

Fig. 6 Distribution of corrosion and cracks for the 'H' specimen with half corrosion.

cracks have been developed on one surface, which was intended in this study.

Figure 9 shows the relationship between the average corrosion weight loss percentage of the rebar over the entire length of the specimen and the number of cracks obtained from the tensile test results.

For the control specimen without any corrosion, three tensile cracks developed, and the number of tensile cracks tended to decrease with an increase in the corrosion weight loss percentage of the rebar. The reason for this outcome is that the corrosion of the rebar resulted in reducing the distribution capacity of the cracks, whereas the length of 80 cm is relatively short such that previously developed transverse corrosion cracks mainly affected the formation of tensile cracks.

3.2 Tension Stiffening Effects of Concrete

Figure 10 shows the tensile stress versus average strain values for the specimens with different levels of corrosion and no corrosion and includes the relationship between the average stress of the concrete and the average strain. The average stress of the concrete was calculated based on the tension stiffening effect of the concrete.

In the 'A' (all) corrosion case, the initial stiffness for specimens A-5 and A-6 with transverse cracks decreased until tensile cracks formed, and the initial peak indicates when the cracking point of the concrete was no longer observed. Moreover, the remaining stress of the concrete at the strain of 0.002 decreased as the corrosion level increased, but the difference is insignificant. In short, when the corrosion level was high, the number of cracks due to stress increased, and the amount of slip that occurred around the transverse cracks increased. Therefore, less displacement in the tensile stress was observed at the time new cracks appeared. However, slip between the rebar and concrete that was caused by longitudinal cracks followed by tensile cracks led to higher average strain values under the same level of stress with an increase in the corrosion level of the rebar.

In the 'H' (half) corrosion case, the tension stiffening effect rapidly decreased due to the increase in steel corrosion when corrosion cracks occurred in concrete specimen H-5.

In the 'C' (center) local corrosion and 'S' (side) local corrosion cases, the decrease in the tension stiffening influences is associated with the steel corrosion, as seen in the relationship between the stress versus average strain values and the concrete stress versus average strain values.

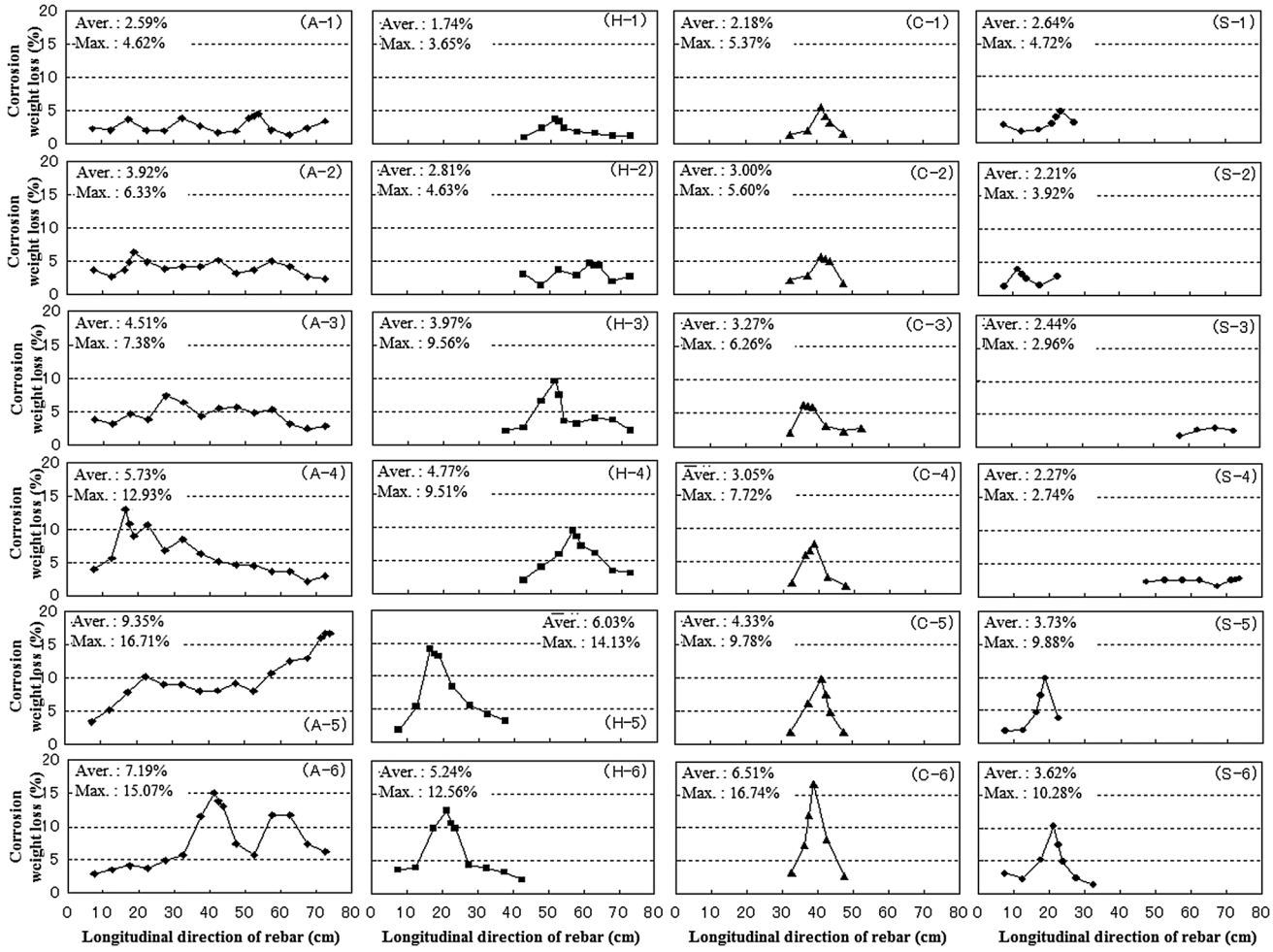

Fig. 7 Corrosion weight loss for each case of corrosion.

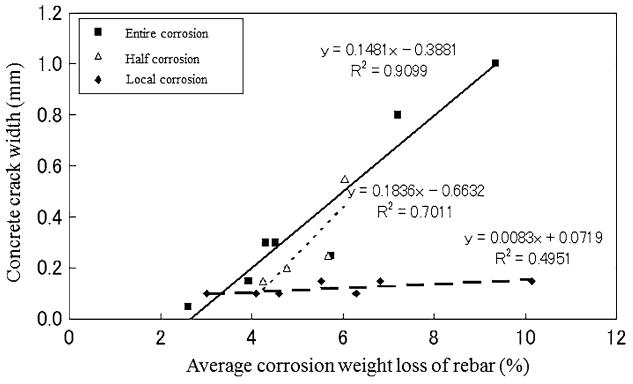

Fig. 8 Average corrosion weight loss percentages versus maximum corrosion cracks.

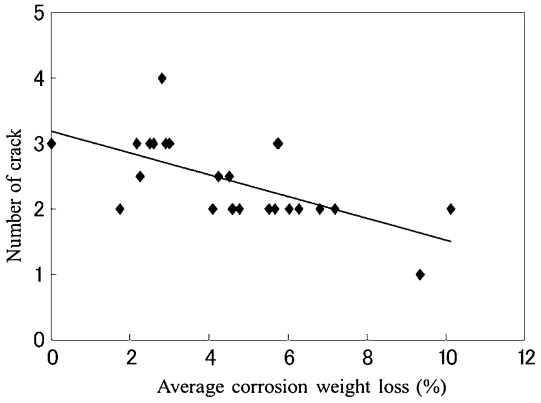

Fig. 9 Tensile cracks with respect to average corrosion weight loss.

However, the stress contribution in the 'C' and "S" corrosion cases was higher than in the 'H' and 'A' corrosion cases.

The deformation of the rebar increased at the cracking point when transverse cracks occurred in the reinforced concrete that was subjected to tensile stress. In addition, deformation increased with the corrosion of the rebar. This outcome was a result of the loss of bond strength due to the steel corrosion and the loss of the cross-section of the reinforcement as well. After the cracks formed, the concrete was hardly affected by the corrosion of the reinforcement, whereas the tension stiffening effects of the concrete with considerable local corrosion apparently decreased.

3.3 Bond Strength and Slip

Slip occurs due to the reduced bond strength between the concrete and the rebar that is induced by developing cracks in the concrete along with expansion that is due to the accumulation of corroded products.

For the finite element analysis in this study, plate bond elements were adopted to model the reinforced concrete with

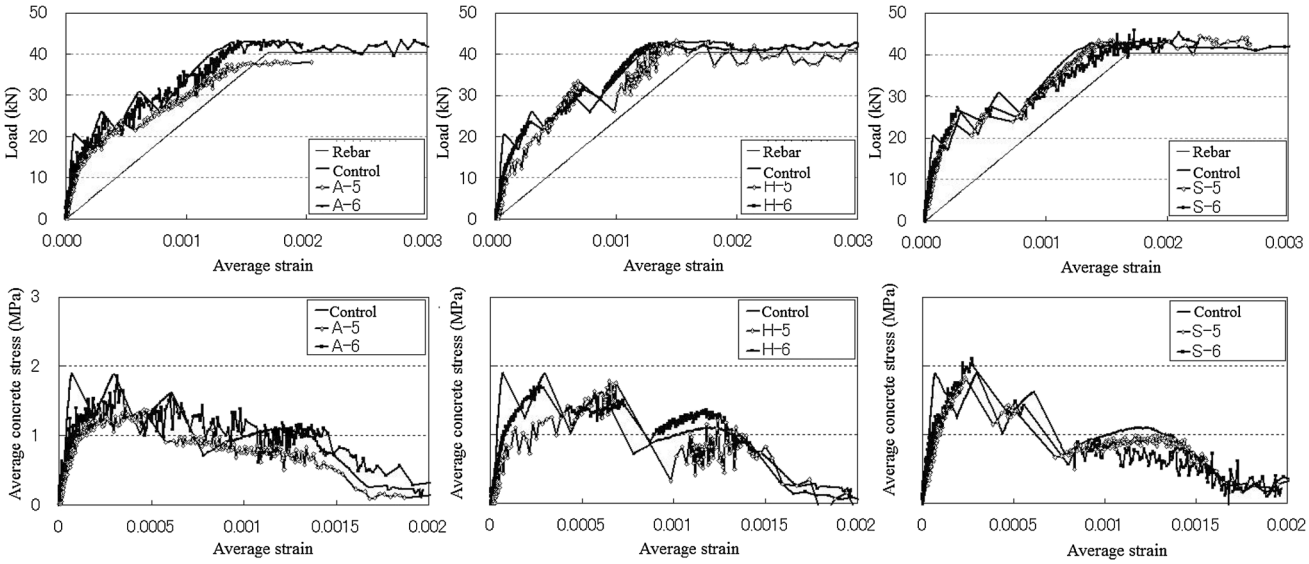

Fig. 10 Average strain versus applied stress.

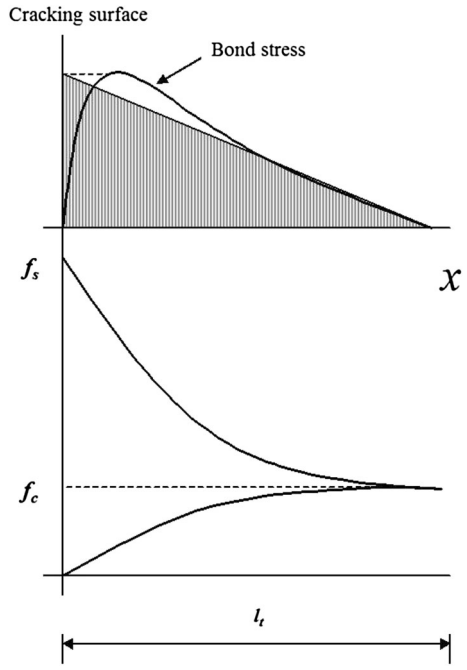

Fig. 11 Distribution of bond stress.

corroded rebar. These bond elements can be presented with bond stress and shear stiffness. The bond strength and slip with respect to the corrosion level must be formulated to determine the bond element of the reinforced concrete with corrosion. Therefore, the force equilibrium condition of the bond force between the rebar and concrete and the tensile force at the concrete crack were used to determine the bond stress. Once a crack due to tensile force develops in the concrete surrounding the rebar, the stress distribution in the concrete and steel is different for various locations, as seen in Fig. 11. The bond stress is the difference between the concrete and rebar in terms of tensile deformation such that the bond stress can be written as Eq. (1):

$$A_c\sigma_{ct} = \pi d_b \int_0^{l_t} \tau_x dx \tag{1}$$

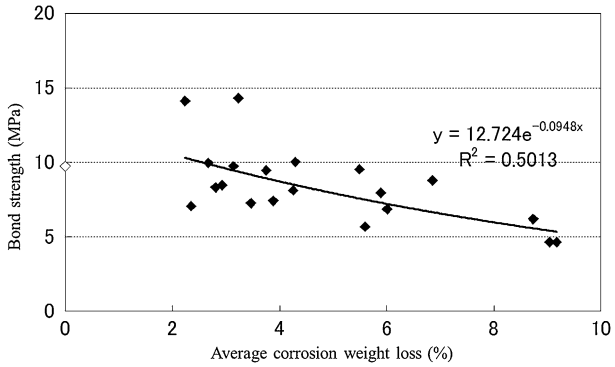

Fig. 12 Bond strength with respect to level of corrosion of rebar.

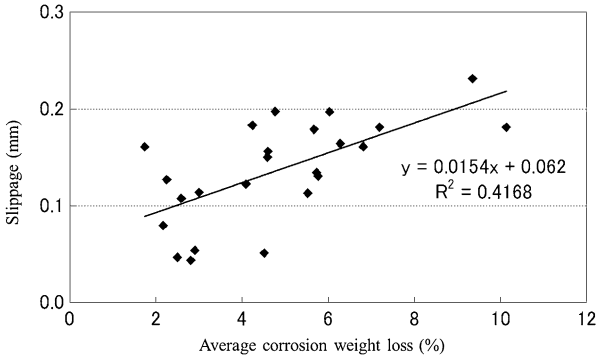

Fig. 13 Slip with respect to level of corrosion of rebar.

where A_c is the cross-section of the concrete, d_b is the diameter of the reinforcement, σ_{ct} is the tensile strength of the concrete (at the crack), τ_x is the bond stress within the transfer length, and l_t is the transfer length of the bond stress.

The force equilibrium is used with linear approximation, as seen in Fig. 11. The bond strength can be calculated using Eqs. (2) and (3).

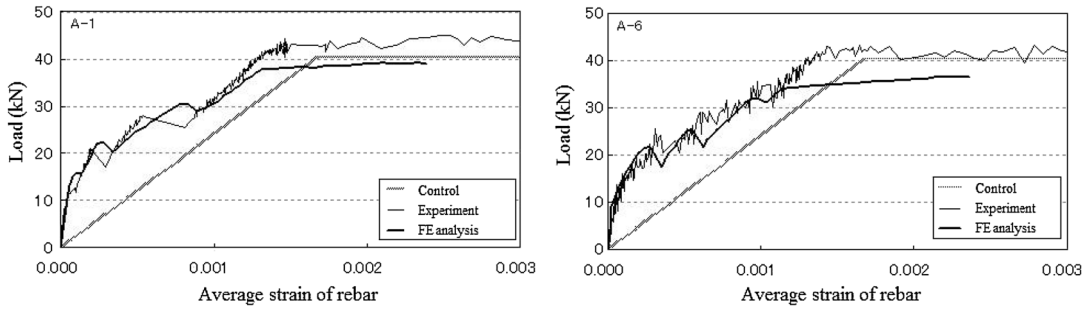

(a) "A" specimens

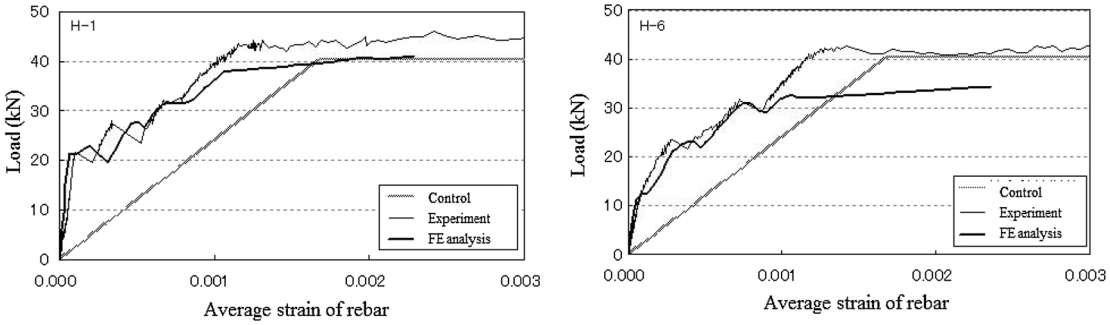

(b) "H" specimens

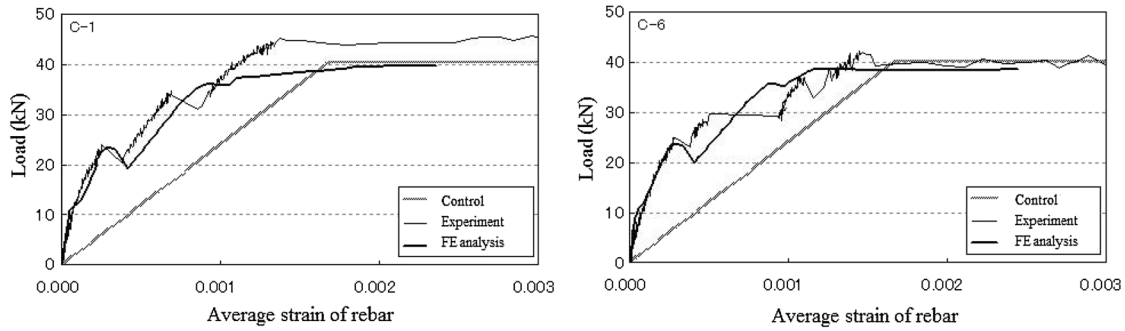

(c) "C" specimens

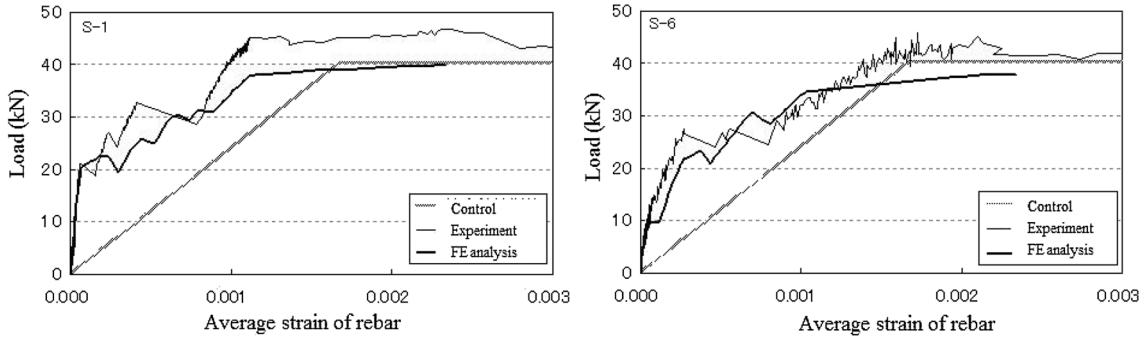

(d) "S" specimens

Fig. 14 Comparison between the experimental results and predicted results by the FE analysis.

$$A_c\sigma_{ct} = \frac{1}{2}\pi d_b l_t \tau_{max} \tag{2}$$

$$\tau_{max} = \frac{2(N+1)A_c\sigma_{ct}}{\pi r L} \tag{3}$$

where N is the number of tensile cracks in the specimen.

Figure 12 shows the relationship between the bond stress and corrosion weight loss of the reinforcement as obtained from the tests. In addition, the bond strength derived from the corrosion weight loss and bond stress can be formulated using Eq. (4).

$$\tau_{c,max} = \tau_{s,max}\left(1.306e^{-0.0948\Delta w}\right) \tag{4}$$

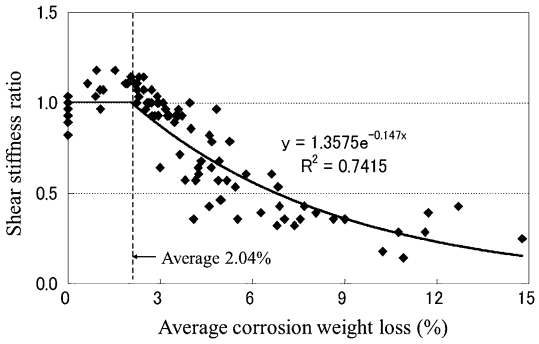

Fig. 15 Relationship between average corrosion weight loss and shear stiffness ratio.

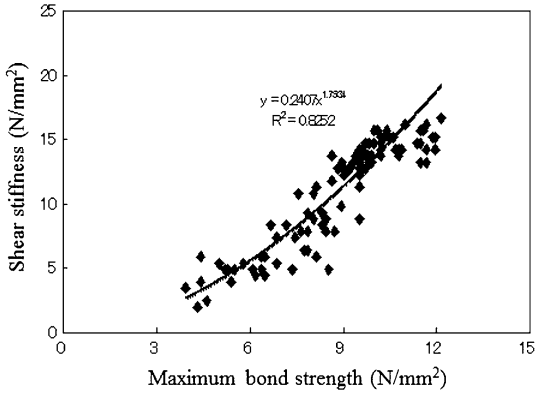

Fig. 16 Relationship between maximum bond strength and shear stiffness.

where $\tau_{c,max}$ is the shear stress of the reinforcement with corrosion (N/mm^2), $\tau_{s,max}$ is the bond stress of the reinforcement without corrosion (N/mm^2), and ΔW is the average corrosion weight loss of the reinforcement (%), ($\Delta W \geq 2.04$ %).

The slip between the rebar and the concrete under tensile stress can be calculated approximately using the widths of the cracks that develop in the concrete (Soltani et al. 2013). The surface deformation of the concrete was ignored in this study. The slip between the rebar and the concrete in the reinforced concrete member is half the maximum crack width according to CEB-FIP Model Code 1990, (1991). Therefore, Eq. (5) can be rewritten as Eq. (6).

$$W_{max} = s_r(\varepsilon_{sm} - \varepsilon_{cm})(l_t \leq S_r \leq 2l_t) \tag{5}$$

$$s(x) = l_t(\varepsilon_s - \varepsilon_c) = \frac{1}{2}S_r(\varepsilon_s - \varepsilon_c) = \frac{W}{2} \tag{6}$$

where W is the crack width and $S(x)$ is the average maximum slip between the reinforcement and the concrete in a reinforced concrete member subjected to tension loading (displacement at a load of 30 kN in this study).

Figure 13 shows the relationship between amounts of slip computed using Eq. (6) and the corrosion weight loss percentage of the rebar. As the corrosion level increases, the slip and relative displacement also increase.

4. Numerical Analysis

4.1 Finite Element Analysis

The relationship between the corrosion weight loss of the rebar and the bond strength, and the relationship between the corrosion weight loss and the slip were determined based on the experimental results of corroded reinforced concrete specimens subjected to tensile stress.

For the finite element (FE) analysis, plate bond elements were adopted to model the reinforced concrete with corroded rebar. These bond elements can be represented as bond stress and shear stiffness. The shear stiffness (D_s) is computed by using the relationship between bond stress (τ_{max}) and shear deformation (γ), which was calculated using slip (s) and the thickness (t) of the bond elements, as shown in Eq. (7).

$$\gamma = \frac{S}{t}, \tau_{\max} = D_s \cdot \gamma \tag{7}$$

In the analysis, the bond element is 0.1-mm thick and the shear stiffness was computed using the data obtained from the experimental results, which include the relationship between the bond stress and slip. The slip obtained from the tests is the average width of the tensile cracks among the several cracks that formed in the specimens. Therefore, the analytical results could be calibrated using the experimental results. Shear stiffness (D_s) values with respect to the corrosion weight loss of the reinforcement were calculated every 10 cm.

Two-dimensional elasto-plastic finite element methods were used in this study. A four-node iso-parametric plate bond element was used for the bond components, and a four-node iso-parametric plane stress element was used for the concrete element. A smeared crack model was used for the cracking of the concrete. After the formation of cracks, the displacement dependent model was used as the orthotropic residual characteristics of the cracks. For the reinforcement, truss elements and Von Mises yield criteria were used in this study. The element size for the longitudinal direction was 2.5 cm, and the concrete element for the lateral direction was 1 cm. The inputs for the material properties of the concrete and reinforcement were based on the test results conducted in this study.

Table 4 Proposed equations for bond element with respect to the level of rebar corrosion.

	Maximum bond strength ($\tau_{s,\ max}$, MPa)	Bond shear stiffness (D_s, MPa)
$0 \leq \Delta W \leq \Delta W_c$	$\tau_{s,max} = 0.34\sigma_B - 1.93$	$D_s = 0.2407(\tau_{max})^{1.7534}$
$\Delta W \geq \Delta W_c$	$\tau_{c,max} = \tau_{s,max}(1.306e^{-0.0948W})$	

4.2 Results of Finite Element Analysis

The shear stiffness values were computed based on the stress-average deformation relationship that is associated with the corrosion level of the reinforcement, which was obtained from the experimental results. Figure 14 shows the comparison between the experimental results and predicted results by the FE analysis. The bond elements model that was used to simulate the experimental results bond elements model adopts a bilinear type. It is possible to apply this model to the specimens regardless of the level of corrosion. The bond elements allow the reduction in bond stress and shear stiffness to be described and computed.

4.3 Proposed Bond Elements

Figure 15 shows the relationship between the shear stiffness values and the level of corrosion of the reinforcement, which is computed with the FE analysis. The average value is 2.04 % of average corrosion weight loss. In addition, bond strength could be calculated with maximum bond strength and shear stiffness relationship (see Fig. 16).

Table 4 shows the proposed equations to determine bond strength and shear stiffness associated with corrosion amount. The bond strength before forming the corrosion cracks can be formulated with concrete compressive strength similarly with the literature by Lee et al. (1996).

5. Conclusions

The following conclusions were drawn based on the limited experimental results found in this study.

(1) In tensile pull-out tests, an increase in corrosion weight loss percentage and fewer cracks adversely affects the dispersion of cracks.
(2) For the "A" specimen, the slope of the ratio of maximum weight loss percentage and average weight loss percentage is 1.87. The ratio values tend to decrease with an increase of the length of corroded area.
(3) The corrosion percentage is about 2.04 % when developing the corrosion cracks. The maximum transverse crack width due to the corrosion increased with an increase of the length of corroded area. The majority of cracks due to the tensile stress are longitudinal direction of rebar. There is no splitting failure even with transverse cracks.
(4) The tensile strength of the concrete tended to decrease due to the corroded rebar with an increase in the length of the corroded area. When the reinforcement corroded without developing cracks in the concrete and with less than 5 % local corrosion, the tensile strength values of those specimens were similar to and/or higher than that of the control specimen. However, the tensile strength decreased considerably when the rebar corrosion level was over 10 %.
(5) When there was no further crack development, the bond strength was calculated using the assumption that the bond strength was distributed linearly between the cracks. A relationship was formulated between the average corrosion level of the rebar in the transfer region of the bond strength.
(6) The bond shear stiffness values were computed and analyzed via finite element analysis that was conducted for the tensile pull-out test results using the relationship between the slip (in terms of the average crack width) and the corrosion level of the rebar. A formula that describes the relationship between the bond shear strength and average corrosion level of the rebar is suggested in this paper.

Acknowledgments

This research was supported by a grant (15RERP-B099826-01) from Residential Environment Research Program funded by Ministry of Land, Infrastructure and Transport of Korean government.

Open Access

References

Al-Hammoud, R., Soudki, K., & Topper, T. H. (2010). Bond analysis of corroded reinforced concrete beams under monotonic and fatigue loads. *Cement & Concrete Composites, 32*(3), 194–203.

Almusallam, A. A., Al-Gahtani, A. S., Aziz, A. R., & Rasheeduzzafar, M. (1996). Effect of reinforcement corrosion on bond strength. *Construction and Building Materials, 10*(2), 123–129.

Auyeung, Y., Balaguru, P., & Chung, L. (2000). Bond behavior of corroded reinforced bars. *ACI Materials Journal, 97*(2), 214–220.

Azad, A. K., Ahmad, S., & Al-Gohi, B. H. A. (2010). Flexural strength of corroded reinforced concrete beams. *Magazine of Concrete Research, 62*(6), 405–414.

Azad, A. K., Ahmad, S., & Azher, S. A. (2007). Residual strength of corrosion-damaged reinforced concrete beams. *ACI Materials Journal, 104*(1), 40–47.

CEB-FIP, CEB-FIP Model Code 1990, (1991) Committee Euro-International Du Beton, Paris, France.

Coronelli, D., & Gambarova, P. (2004). Structural assessment of corroded reinforced concrete beams: modeling guidelines. *Journal of Structural Engineering, 130*(8), 1214–1224.

Dekoster, M., Buyle-Bodin, F., Maurel, O., & Delmas, Y. (2003). Modeling of the flexural behaviour of RC beams subjected to localized and uniform corrosion. *Engineering Structures, 25*(10), 1333–1341.

Imam, A., Anifowose, F., & Azad, A. K. (2015). Residual of corroded reinforced concrete beam using and adaptive model based on ANN. *International Journal of Concrete Structures and Materials, 9*(2), 159–172.

Kim, H. R. (2008). An evaluation study on the degradation of the load-bearing capacity by the rebar corrosion in reinforced concrete structures. Ph.D. Thesis. University of Tokyo, Tokyo, Japan.

Kim, H. R., Nagai, H., & Noguchi, T. (2008). Bond characteristics of reinforced concrete with corroded rebar in axially-loaded tension tests. *In Proceedings of the Japan Concrete Institute, 30*(1), 1101–1106.

Lee, H. S., Tomosawa, F., & Noguchi, T. (1996). Effects of rebar corrosion on the structural performance of singly reinforced beams. *Durability of Building Materials and Components, 7*(1), 571–580.

Soltani, A., Harries, K. A., & Shahrooz, B. M. (2013). Crack opening behavior of concrete reinforced with high strength reinforcing steel. *International Journal of Concrete Structures and Materials., 7*(4), 253–564.

Stewart, M. G. (2004). Spatial variability of pitting corrosion and its influence on structural fragility and reliability of RC beams in flexure. *Structural Safety, 26*(4), 453–470.

Yang, S., Fang, C. Q., Yuan, Z. J., & Yi, M. Y. (2015). Effects of reinforcement corrosion and repeated loads on performance of reinforced concrete beam. *Advances in Structural Engineering, 18*(8), 1257–1271.

Yoon, S., Wang, K., Weiss, W. J., & Shah, S. P. (2000). Interaction between loading, corrosion, and serviceability of reinforced concrete. *ACI Materials Journal, 97*(6), 637–644.